Electrolyte Effects of Poly(3-methylthiophene) via PET/ITO and Synthesis of 5-(3,6-Di(thiophene-2-yl)-9*H*-carbazole-9-yl) Pentanitrile on Electrochemical Impedance Spectroscopy

Murat Ates,[1] Tolga Karazehir,[1,2] Nesimi Uludag[1]

[1]*Department of Chemistry, Faculty of Arts and Sciences, Namik Kemal University, Degirmenalti Campus, 59030 Tekirdag, Turkey*
[2]*Department of Chemistry, Istanbul Technical University, Polymer Science and Technology, Maslak, 34469 Istanbul, Turkey*

Received 30 September 2011; accepted 27 November 2011
DOI 10.1002/app.36581
Published online 1 February 2012 in Wiley Online Library (wileyonlinelibrary.com).

ABSTRACT: In this article, 3-methylthiophene (3MTh) and 5-(3,6-di(thiophene-2-yl)-9H-carbazole-9-yl) pentanitrile (ThCzpN) comonomer were electrochemically deposited on poly(ethylene terephthalate)/indium tin oxide (PET/ITO) electrode and carbon fiber micro electrode (CFME) in sodium perchlorate ($NaClO_4$)/acetonitrile (ACN), respectively. ThCzpN comonomer was characterized by ^{1}H-nuclear magnetic resonance spectroscopy and Fourier transform infrared spectroscopy (FTIR) analysis. Poly(ThCzpN)/CFME is characterized by cyclic voltammetry (CV), Scanning electron microscopy-energy dispersive X-ray analysis (SEM-EDX), and electrochemical impedance spectroscopy (EIS). The detailed characterization of the resulting electrocoated poly(3MTh) on PET/ITO thin films was studied by different techniques, i.e., CV and EIS. The effects of electrolytes after electrocoated of modified electrodes were examined by EIS technique in various electrolytes medium (sodium perchlorate ($NaClO_4$), lithium perchlorate ($LiClO_4$), tetraethyl ammonium tetrafluoroborate ($TEABF_4$), and tetrabutyl ammonium tetrafluoroborate ($TBABF_4$)/acetonitrile (ACN) solution). Capacitive behaviors of modified PET/ITO electrode were defined via Nyquist, Bode-magnitude, Bode-Phase, and admittance plots. Variation of capacitance values by various electrolytes and low-frequency capacitance (C_{LF}) values are presented. C_{LF} value electrocoated polymer thin film by CV method in the 0.1*M* $NaClO_4$ electrolyte with a charge of 7.898 mC was obtained about 59.1 mF cm^{-2}. The highest low-frequency capacitance (C_{LF}) was obtained from the Nyquist plot with $[ThCzpN]_0$ = 3 m*M* as 0.070 mF cm^{-2}. Equivalent circuit model [R(QR(CR)(RW))(CR)] was suggested for poly(3MTh) on PET/ITO in four different electrolytes medium. © 2012 Wiley Periodicals, Inc. J Appl Polym Sci 125: 3302–3312, 2012

Key words: coatings; electrochemistry; thin films; surface modification; functionalization of polymers

INTRODUCTION

Conducting polymers (CPs) have been attracted more attention because of its exhibit good stabilities, conductivities, and ease of synthesis.[1,2] Among CPs, poly(3-methylthiophene) poly(P3MTh) and its derivatives that are environmentally stable both in their doped and undoped states.[3] Furthermore, poly(3-alkylthiophenes), (P3ATs) have been substituted into the 3-position of the thiophene ring has led to highly processable polymers.[4] P3ATs containing relatively long alkyl chains highly soluble,[5] which makes them particularly attractive for technological applications[6–9] because of their remarkable solid-state properties including thermochromism, electrochromism, luminescence, and photoconductivity.[10]

Cyclic voltammograms obtained during the switching of poly(3MTh) between reduced and oxidized states are generally known to exhibit a single prominent oxidation peak followed by a high residual current tail.[11] Previous works[12,13] have shown that the voltammograms of poly(3MTh) in aqueous electrolytes are strongly dependent upon the types of anions present in the solution. Ates has studied Poly(3MTh)/carbon fiber microelectrode (CFME) in 0.1*M* $NaClO_4$/ACN.[14] It shows high low-frequency capacitance of $\sim$ 4.12 F g^{-1} in the initial monomer concentration of 0.1*M*. Poly(3MTh) has been used various application, such as biosensor,[15] lithium-ion battery,[16] field-effect transistors,[17] photovoltaic device etc.[18] Marque et al.[19] synthesized poly(3MTh) as thin films using PF_6^-, ClO_4^-, BF_4^-, $CF_3SO_3^-$ as the

Correspondence to: M. Ates (mates@nku.edu.tr).
Contract grant sponsor: Research Foundation of Namik Kemal University; contract grant number: NKU.BAP.00.10.AR.11.01.
Contract grant sponsor: Scientific & Technological Research Council of Turkey (TUBITAK); contract grant number: TBAG-110T516.

doping anion and Li^+ and Bu_4N^+ as the counter-cation. They demonstrated an anion effect that could be related to the geometrical parameters of the ion by replacing the anion after synthesis, and influence of the anion occurs during the synthesis of the polymer and determines its structure. Refaey[20] studied the electrochemical properties of poly(3MTh) films galvanostatically synthesized by using BF_4^-, ClO_4^-, $CF_3SO_3^-$ as doping anion and Li^+ as cation on polished Pt wire electrode. Electrochemical impedance spectroscopic (EIS) measurements in a wide frequency range were used. Results showed that the nature of the anion plays a major role on the electrochemical behavior of the polymer, and basis of models developed for intercalation electrodes in relation to the geometry and morphology of the polymer electrode. EIS has become an increasingly popular electrochemical technique for the investigation of bulk and interfacial electrical properties of any kind of solid or liquid material.[21] It may be used to investigate the dynamics of bound or mobile charge in the bulk or interfacial regions of any kind of solid or liquid material: ionic, semiconducting, mixed electronic ionic, and even insulators.[22] The doping/undoping processes during the overall redox reactions of this kind of polymers have been studied by means of electrochemical techniques. EIS has revealed during the last few years as one of the most powerful and preferred techniques to obtain relevant information about the electrical properties of CPs. From an appropriate theoretical model and with the help of the mathematical software tools it is possible to obtain information about many physical properties of these polymers.[23]

In previous study, PET/ITO substrates was used for electrochromic devices. Lin et al. investigated electrochromic properties of nickel oxide (NiO_x),[24] WO_xC_y,[25] nickel-vanadium oxide (NiV_xO_y),[26] tungsten oxide (WO_{3-z})[27] thin films sputtered on flexible PET/ITO substrates. PET/ITO substrates were used for glucose biosensor by Li et al.[28] based on a SnO_2/ITO/PET. Miettunen et al.[29] used PET/ITO substrate for dye solar cells; atomic-layer-deposited TiO_2 recombination blocking layers were prepared on PET/ITO photo-electrode substrates.

In this study, 3-methyl thiophene on PET/ITO electrode and 5-(3,6-di(thiophene-2-yl)-9H-carbazole-9-yl) pentanitrile/CFME was electropolymerized in Sodium perchlorate ($NaClO_4$)/Acetonitrile (ACN). Poly(3MTh)/PET/ITO was performed in various electrolytes, 0.1*M* Sodium perchlorate ($NaClO_4$), Lithiumperchlorate ($LiClO_4$), Tetraethylammonium tetrafluoroborate ($TEABF_4$), and Tetrabutylammonium tetrafluoroborate ($TBABF_4$)/Acetonitrile (ACN) solution. Poly(ThCzpN)/CFME was studied in various initial monomer concentrations (1, 2 and 3 mM). EIS of electrocoated 3MTh was studied using circuit model of [R(QR(CR)(RW))(CR)].

EXPERIMENTAL

Materials

3-methylthiophene (3MTh) (>95%), lithium perchlorate, and sodium perchlorate (>98%), tetraethyl ammonium tetrafluoroborate (>97%), and tetrabutylammonium tetrafluoroborate (>97%), 3,6-dibromocarbazole (>99%), thiophene (>99%), and 5-choloropentanitrile (>99%) were obtained from Sigma-Aldrich. Flexible PET/ITO substrates (working electrode diameter = 0.25 cm^2) were purchased from Sheldahl, Northfield, MN. Tetrahydrofuran, sodium hydroxide, silica gel (60 F254), acetonitrile, and dichloromethane were purchased from Merck. Sodium perchlorate (>98%), *n*-butyl lithium, $NiCl_2$, $MgBr_2.Et_2O$, petroleum ether, and chloroform were obtained from Fluka. All chemicals were analytical grade reagents and were used as received.

Instrumentation

^{1}H-NMR spectrum was recorded on a Varian Gemini 300 spectrometer, operating at 300 MHz. Spectrum was registered in $CDCl_3$ using the solvent as internal standard at 300 MHz for ^{1}H at room temperature. Chemical shifts are expressed in terms of parts per million (δ) and the coupling constants are given in Hz. Cyclic voltammetry (CV) was performed using a PARSTAT 2263-1 and 2273 (software, powersuit, and Faraday cage, BAS Cell Stand C_3) in a three-electrode electrochemical cell employing PET/ITO and CFME as the working electrode, platinum wire as the counter electrode, and Ag/AgCl (3*M*) as the reference electrode.

Electrocoated CFMEs were characterized by FTIR reflectance spectroscopy (Perkin Elmer, Spectrum One B, with an ATR attachment Universal ATR-with ZnSe crystal). Modified CFMEs were washed in solvent of acetonitrile. The films of polymers, electrocoated onto carbon fibers were analyzed by scanning electron microscopy using a LEO 1430 VP model SEM. The excitation energy was 5 keV. Average values of the increase in thickness were obtained via SEM images taking into account the diameter of the uncoated fiber. The diameters for the fibers represent an average of 5–6 measurements on carbon fiber.

Electrochemical impedance spectroscopy (EIS)

The EIS measurements were taken at room temperature (23 ± 2°C) using a conventional three electrode cell configuration. EIS measurements were conducted in monomer-free electrolyte solution with a perturbation amplitude 10 mV over a frequency range of 10 mHz to 100 kHz with PARSTAT 2263-1 and 2273 (software; powersuit).

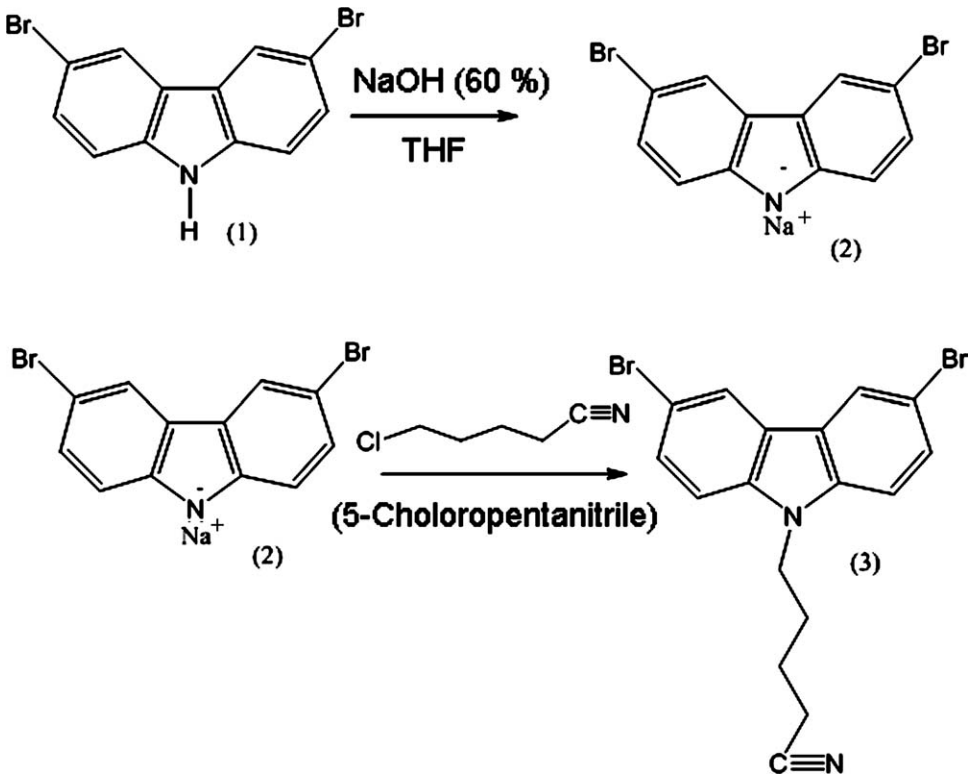

Figure 1 Synthesis way of 5,(3,6-dibromo-9H-carbazole-9-yl) pentanitrile.

Preparation of the carbon fiber microelectrodes

High strength (HS) carbon fibers C320.000A (CA) (Sigri Carbon, Meitingen, Germany) containing 320,000 single filaments in roving and high modulus (HM) carbon fibers were used as working electrodes. The preparation of CFME was given in our previous articles.[30,31] All of the electrodes were prepared using a 3 cm long bundle of the CFME (with average diameter of around 7 μm) attached to a copper wire with a Teflon tape. A number of carbon fibers in the bundle were about ~ 10. One centimeter of the CFME was dipped into the solution to keep the electrode area constant (~ 0.022 cm^2) and the rest of the electrode was covered with a Teflon tape. The CFMEs were firstly cleaned with acetone and then dried with an air-dryer before the experiments.[32]

RESULTS AND DISCUSSION

Synthesis of 5-(3, 6-dibromo-9*H*-carbazole-9-yl) pentanitrile

3,6-dibromo-carbazole (5.0 g, 15.38 mmol) was dissolved in 250 mL tetrahydrofuran at room temperature by magnetic stirrer. During the mixture process, sodium hydroxide (NaOH) (1.2 g, 30.76 mmol, 60%) was added slowly under nitrogen atmosphere at 80°C in 2 h. After completion the reaction, 5-chloropentanitrile (3.6 mL, 30.76 mmol, 98%) was added the sodium salt under nitrogen atmosphere at 100°C in ~ 6 days. Then the mixture was poured into cold water and dichloromethane. The solvent was evaporated and the residue was purified by silica gel chromatography and crystallized from 10% HCl. Purification was supplied by column chromatography with petroleum ether-chloroform (2 : 1). 5-(3, 6-dibromo-9H-carbazole-9-yl) pentanitrile was obtained as white color crystal (4 g, 80%, $R_f = 0.76$ (CH_2Cl_2), melting point: 154°C). The synthesis way was given in Figure 1.

^{1}H-NMR ($CDCl_3$): δ 8.3–7.2 (m, 6H, aromatic C—H), 4,3 (*t*, CH_2), 1, 2–2.4 (m, CH_2CH_2) (Fig. 2).

FTIR (Solid KBr): ν 3100 cm^{-1} 3000, (aliphatic CH), 2250 (C≡N) cm^{-1}, 1609 cm^{-1}, 1451, 1329 cm^{-1} (aromatic C=C) (Fig. 3).

Synthesis of 5-(3,6-di(thiophene-2-yl)-9*H*-carbazole-9-yl) pentanitrile comonomer

Thiophene (2.4 mL, 30 mmol) was dissolved in 100 mL THF under nitrogen atmosphere with the help of inside methanol-liquid nitrogen mixture at −76°C. *n*-butyl lithium was added by injection to the mixture (20 mL, 24.3 mmol). After 1 h, reaction temperature adjusted at 0°C and one portion of $MgBr_2.Et_2O$ (0.78 g) was added to the mixture. And then, 5-(3,6-dibromo-9H-carbazole-9-yl) pentanitrile (1.77 g, 4.35

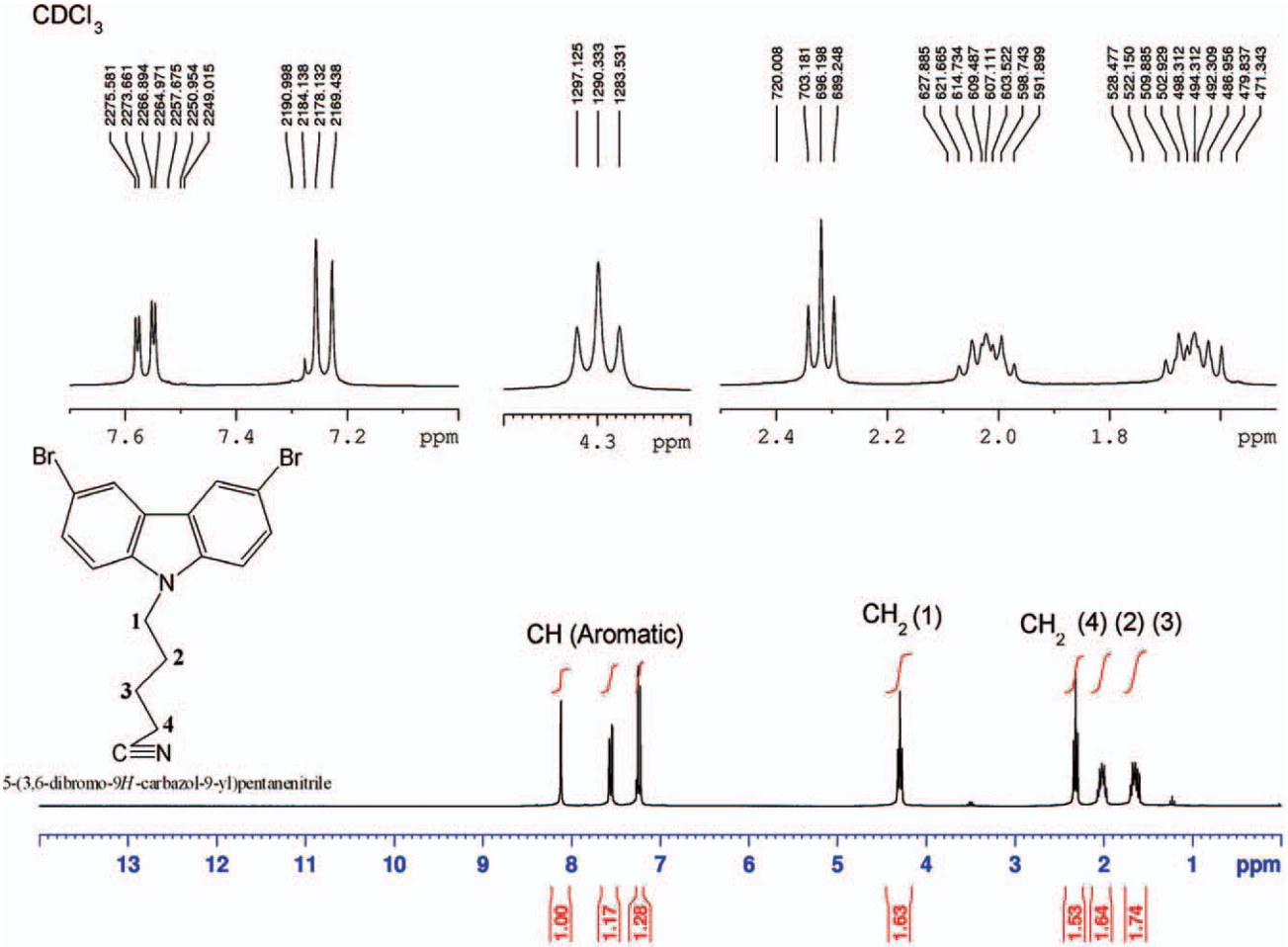

Figure 2 ^{1}H-NMR spectrum of 5,(3,6-dibromo-9H-carbazole-9-yl) pentanitrile. [Color figure can be viewed in the online issue, which is available at wileyonlinelibrary.com.].

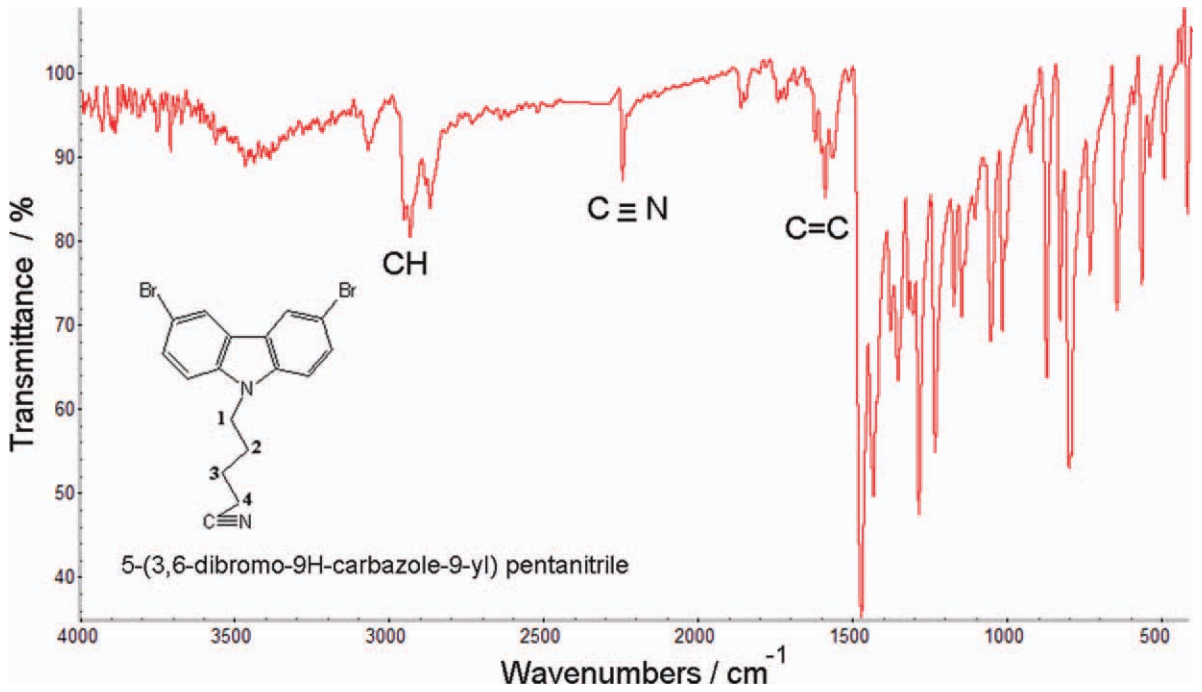

Figure 3 FTIR spectrum of 5,(3, 6-dibromo-9H-carbazole-9-yl) pentanitrile. [Color figure can be viewed in the online issue, which is available at wileyonlinelibrary.com.].

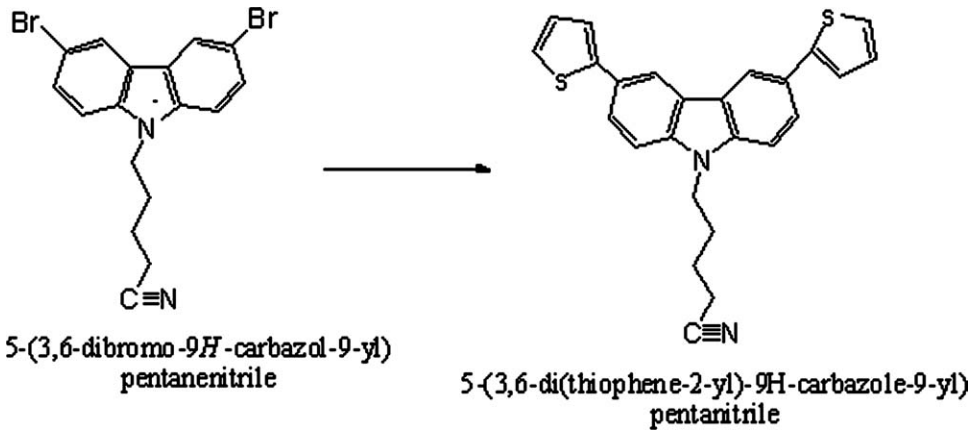

Figure 4 Synthesis way of 5,(3,6-di(thiophene-2-yl-carbazole-9-yl) pentanitrile.

mmol) and $NiCl_2$ (0.5 g, 0.92 mmol) were dissolved in 30 mL THF solution and added to the mixture. Reaction was continued ~ 45 h at room temperature. The solvent was evaporated and the residue was purified by silica gel chromatography and crystallized from 60% NaOH and CH_2Cl_2. The target substance of 5-(3,6-di(thiophene-2-yl)-9H-carbazole-9-yl) pentanitrile comonomer was obtained successfully (Fig. 4).

FTIR (Solid KBr): ν 3042 (aromatic C—H), 2932 (aliphatic C—H), 1719 (CN), 1447, 1325 cm^{-1} (aromatic C=C).

^{1}H-NMR ($CDCl_3$): δ 8.1–8.0 (d, 2H aromatic CH), 7.472–7.16 (m, 10H, aromatic CH), 4.38–4.23 (m, 2H CH_2), 2.35–1.37(m, 6H CH_2).

Electropolymerization of 3-methylthiophene on PET/ITO electrode and 5-(3,6-di(thiophene-2-yl)-9*H*-carbazole-9-yl) pentanitrile on CFME

Electropolymerization process was achieved by CV method. Electrogrowth of 3MTh on PET/ITO was shown in Figure 5(a). Electropolymerization experiments were done at a scan rate of 5 mV s^{-1} in 0.1*M* $NaClO_4$/ACN containing initial monomer concentration of 10 m*M* in the potential ranges from 0.00 to 2.0 V at room temperature. Figure 5(a) also shows that the values of Ep_a and Ep_c are between 0.43 and 0.47 V, respectively.

Multisweep cyclic voltammogram of ThCzpN/CFME in the initial monomer concentration for 3 m*M* [Fig. 5(b)] in 0.1*M* $NaClO_4$/ACN show an increasing current density with each cycle (Ep_a = 1.26 V; Ep_c = 1.02 V), respectively. Many functional polymers, such as 9-tosyl-9H-carbazole (TsCz),[33] 9-(4-vinylbenzyl)-9H-carbazole,[34] have been previously electro-synthesized on CFME. The peak separation between anodic and cathodic peak potentials (Δ*E*) during polymer growth was obtained in the initial monomer concentration of 10 m*M* at a potential value of 0.1 V. Therefore, both the peak separation between anodic and cathodic peak potentials (ΔE = 0.04 V) and the anodic and cathodic peak current density ratio (i_a/i_c = 0.97) show the reversible modified PET/ITO electrode. The separation between anodic and cathodic peaks is associated with ion transport resistance involved in these redox reactions.[35] It gives information about polymer thickness that is, if polymer thickness is high, electron transfer between polymer and electrolyte will be slow. Thus, Δ*E* can serve as an indication for resistance of ion migration in the electrode.[36] The value of Δ*E* generally increases with the amount of polymer film on the electrode. This is expected since an increase in polymer film thickness leads to an increase in resistance for ion penetration.[37] Electrochemically modified polymer electrodes showed linear dependency between scan rate and current density that means polymer electrode processes are thin film formation. Electro-activity of polymer electrodes is the highest for poly(3MTh) synthesized in the initial monomer concentration of 10 m*M*.

Effect of scan rate in monomer-free solution

Poly(3MTh) on PET/ITO film was inserted into monomer-free electrolyte solution and its redox behavior was studied. One oxidation and one reduction peaks were observed by increasing the applied potential. This anodic process at ~ 0.93 V is associated with one cathodic wave occurring at ~ +0.85 V by reverse scans at 10 mV s^{-1}. A reversible cyclic voltammogram is generally only observed if both the oxidized and reduced species are stable and the kinetic of the electron transfer process is fast. The peak current (i_p) for a reversible voltammogram at 25°C is given using the Randles-Sevcik equation[38]: $i_p = (2.69 \times 10^5) \times n^{3/2} \times A \times D^{1/2} \times C_0 \times \nu^{1/2}$ where ν is the scan rate, *A* is electrode area, *D* is the diffusion coefficient of electro-active species in the solution. The scan rate dependence of the anodic

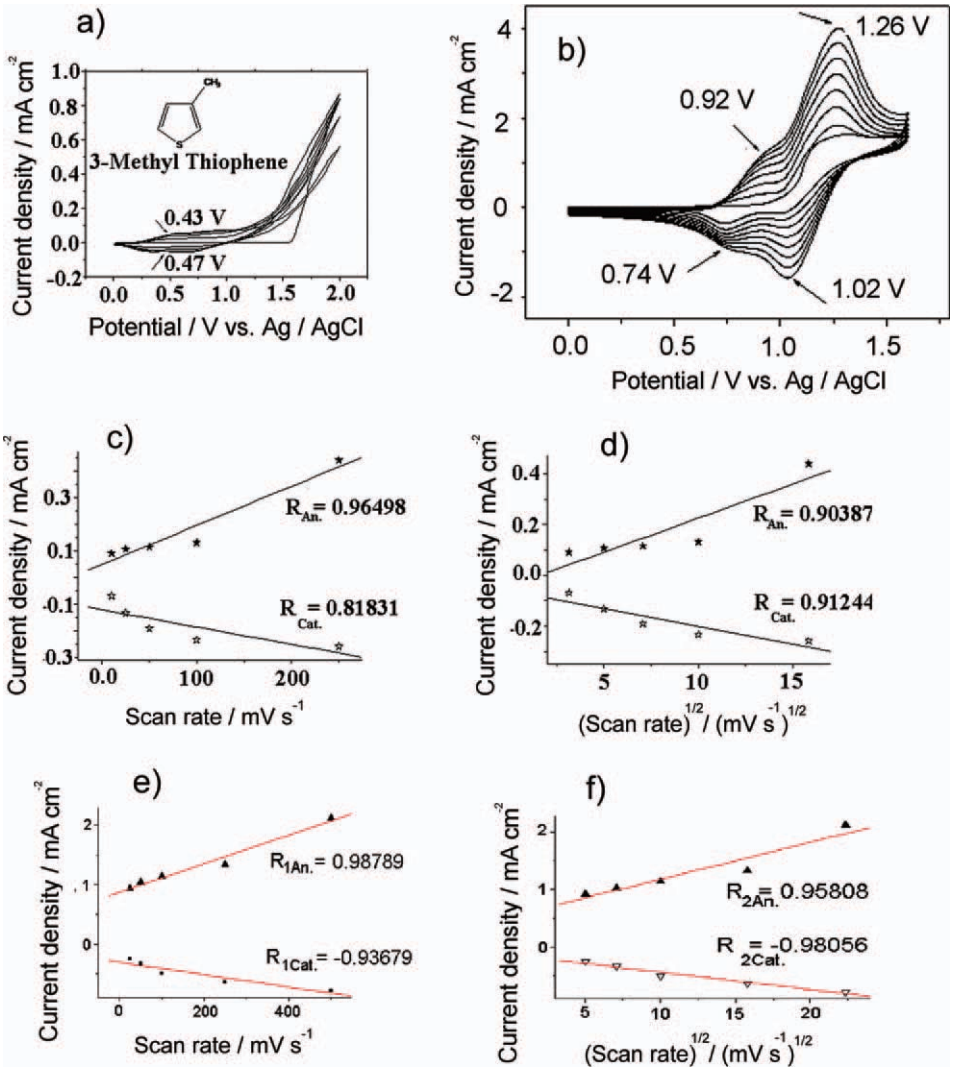

Figure 5 (a) Electrogrowth of poly(3MTh) on PET/ITO. Polymerization conditions: Q = 7.898 mC, $[3MTh]_0$ = 10 m*M*, scan rate = 5 mV s^{-1}, (b) Poly(ThCzpN) on CFME, $[ThCzpN]_0$ = 3 m*M*, ΔQ = 2.815 Mc, in 0.1*M* $NaClO_4$/ACN at a scan rate of 100 mV s^{-1}. Using multiple (8 cycles) and potential range: 0–1.6 V. (c) Plots of anodic and cathodic peak current density versus scan rate dependence of Poly(3MTh) thin film in monomer-free solution in 0.1*M* $NaClO_4$/ACN. (d) Plots of anodic and cathodic peak current density versus the square root of scan rate dependence of poly(3MTh) on PET/ITO thin film in monomer-free solution in 0.1*M* $NaClO_4$/ACN. (e) Plots of anodic and cathodic peak current density versus scan rate dependence of Poly(ThCzpN) thin film in monomer-free solution in 0.1*M* $NaClO_4$/ACN. (f) Plots of anodic and cathodic peak current density versus the square root of scan rate dependence of poly(ThCzpN) on CFME thin film in monomer-free solution in 0.1*M* $NaClO_4$/ACN. Scan rates were given from 25 to 500 mV s^{-1}. [Color figure can be viewed in the online issue, which is available at wileyonlinelibrary.com.].

and cathodic peak currents shows a parabola dependence on scan rate (R_{an} = 0.96498 and R_{cat} = −0.81831) for poly(3MTh) [Fig. 5(c)] and (R_{an} = 0.98789 and R_{cat} = −0.93679) for poly(ThCzpN) against ν Figure 5(e). Peak current density is proportional to $\nu^{1/2}$ in the range of scan rates (Regression coefficient (R_{an} = 0.90387 and 0.95808 and R_{cat} = −0.91244 and −0.98056) where diffusion control applies[39] for poly(3-methylthiophene) and poly(ThCzpN), respectively as given in Figure 5(d,f). This demonstrates that the electrochemical process probably has both diffusion controlled process and thin film formation.[40] The polymerization process was applied at 100 mV s^{-1} at which the anodic and cathodic peaks were well-defined, but at higher scan rates (such as 500 mV s^{-1}), the peaks were broader and less well-defined.

SEM-EDX analysis of poly(ThCzpN)

SEM images of poly(ThCzpN) proves electrodeposition process of 5-(3,6-di(thiophene-2-yl)-9H-carbazole-9-yl) pentanitrile on CFME. Coating thickness for carbon fiber depends on the charge passed through the fibers; an increase of charge increased thickness. So, the highest charge obtained for initial

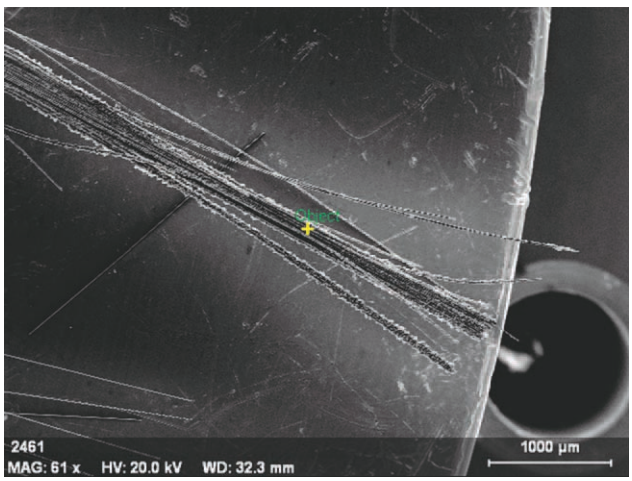

Figure 6 SEM images of (a) Poly(ThCzpN)/CFME. Experimental conditions are 8th cycles, at a scan rate of 100 mV s^{-1}, $[ThCzpN]_0 = 1$ m*M* in 0.1*M* $NaClO_4$/ACN. [Color figure can be viewed in the online issue, which is available at wileyonlinelibrary.com.].

monomer concentration of $[ThCzpN]_0 = 1$ m*M* was taken as shown in Figure 6.

EDX image of point analysis was added to proof the alternating copolymer formation on CFME (Fig. 7). The presence of O, Na, and Cl element's peaks indicate the inclusion of dopant anion (ClO_4^-) of the supporting electrolyte into copolymer structure during electro-growth process.[41]

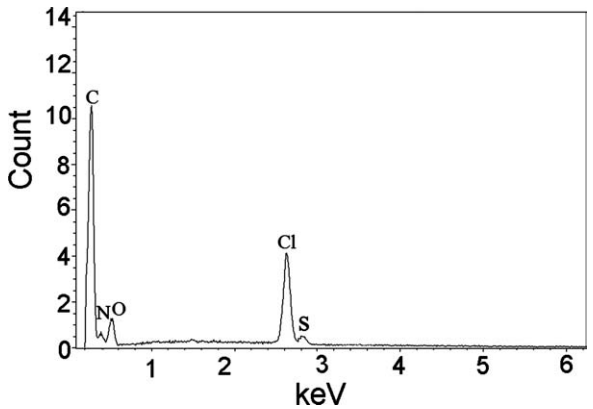

Figure 7 EDX-point analysis of Poly(ThCzpN)/CFME was taken from SEM measurements, $[ThCzpN]_0 = 1$ m*M* in 0.1*M* $NaClO_4$/ACN.

Electrochemical impedance spectroscopy

All electrodes show a significant deviation from the capacitive line (*y*-axis) in impedance spectra, indicating fast charge transfer at the PET/ITO/poly(3MTh)/solution interfaces, as well as fast charge transport in the polymer bulk. The increase in *Z*″ from Nyquist plot was given in Figure 8(a–d). The lowest frequency (*f*) and the highest *Z*″ values are placed in the formula of; $C_{LF} = 1/2\pi \times f \times z''$ for specific capacitance calculations.[42] Nyquist plot for poly(3MTh) indicates the highest C_{LF} values at the frequency of 10 mHz for $NaClO_4$/ACN as 59.1 mF

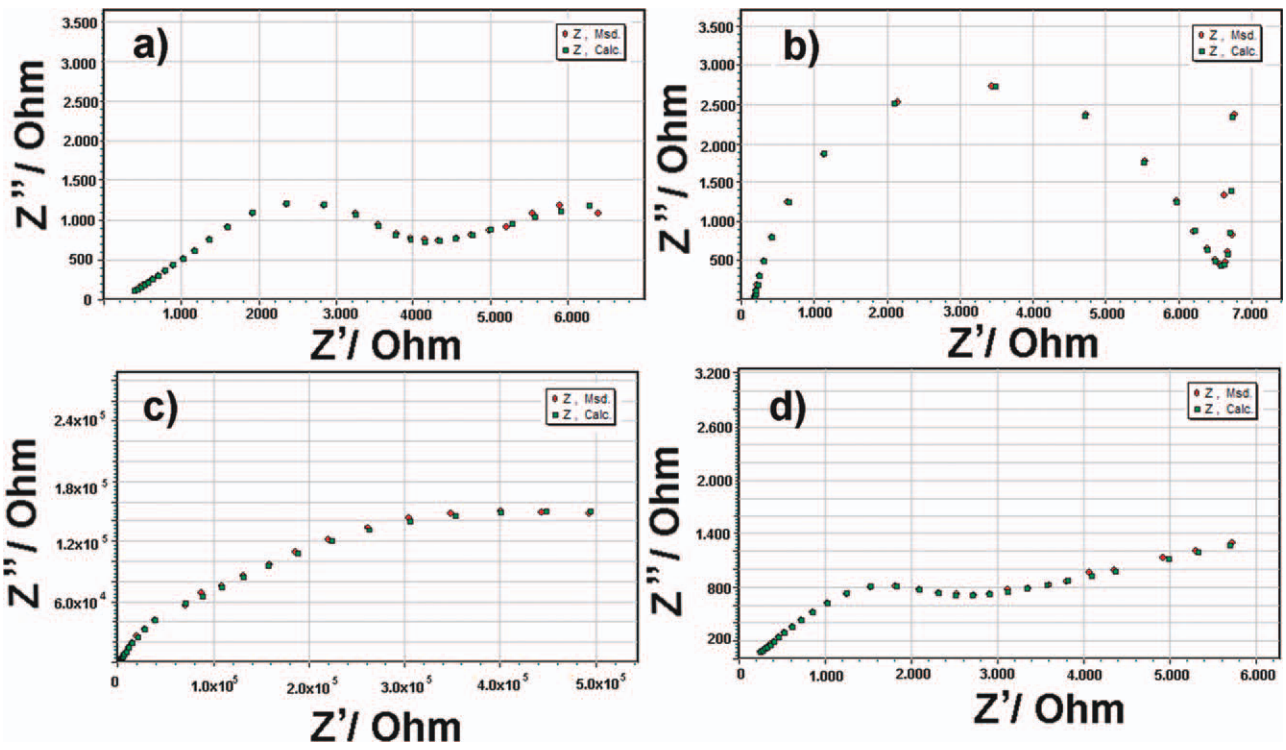

Figure 8 Nyquist plots for Poly(3MTh) electrocoated on PET/ITO. (a) 0.1*M* $LiClO_4$/ACN, (b) 0.1*M* $NaClO_4$/ACN, (c) 0.1*M* $TBABF_4$/ACN, and (d) $TEABF_4$/ACN, $[3MTh]_0 = 10$ m*M*.

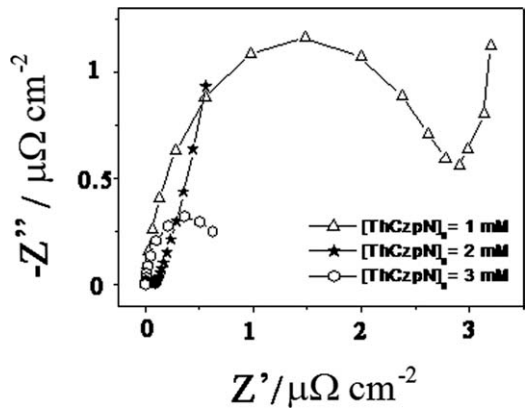

Figure 9 Nyquist plot for poly(ThCzpN) electrocoated on CFMEs. Plots were taken for $[ThCzpN]_0$ = 1, 2, and 3 m*M*.

cm^{-2} in the initial monomer concentration of 10 m*M* [Fig. 8(b)]. The other C_{LF} values are calculated as 58.7 mF cm^{-2} for $LiClO_4$/ACN [Fig. 8(a)]; 0.43 mF cm^{-2} for $TBABF_4$/ACN [Fig. 8(c)]; 56.6 mF cm^{-2} for $TEABF_4$/ACN [Fig. 8(d)].

The highest low-frequency capacitance (C_{LF}) was obtained from the Nyquist plot with $[ThCzpN]_0$ = 3 m*M* as 0.070 mF cm^{-2}. This may be related to lowest electro-deposition charge (2.815 mC) during electrocopolymerization process (Fig. 9).

A value of double layer capacitance, C_{dl}, can be calculated from a Bode-magnitude plot, by extrapolating the linear section to value $\omega = 1$ ($\log w = 0$), employing the relationship $IZI = 1/C_{dl}$ as shown in Figure 10(a–d). The highest double layer capacitance (C_{dl} = 17.6 μF cm^{-2}) was obtained for poly(3MTh) for $NaClO_4$/ACN in the initial monomer concentration of 10 m*M* [Fig. 10(b)]. The other electrolytes C_{dl} values are calculated as 4.42 μF cm^{-2} for $LiClO_4$/ACN [Fig. 10(a)]; 0.58 μF cm^{-2} for $TBABF_4$/ACN [Fig. 10(c)]; 4.94 μF cm^{-2} for $TEABF_4$/ACN [Fig. 10(d)]. Bu_4N^+ is a large cation (radius ($r_{Bu4N}{}^+$) = 0.513 nm), poorly solvated in acetonitrile; however, Na^+ ($r_{Na}{}^+$) = 180 pm and Li^+ ($r_{Li}{}^+$) = 167 pm, largely solvated, is more mobile than the tetrabutylammonium ion. Therefore, C_{dl} *v*alues of Na^+ and Li^+ are considerable higher than $TEABF_4$ and $TBABF_4$.

At the maximum phase angle for poly(3MTh) in the initial monomer concentrations of 10 m*M* was obtained as ~ 62.3° for $NaClO_4$/ACN at the frequency of 50 Hz [Fig. 10(b)]. Therefore, the reason of the highest maximum phase angle is the higher *n* =

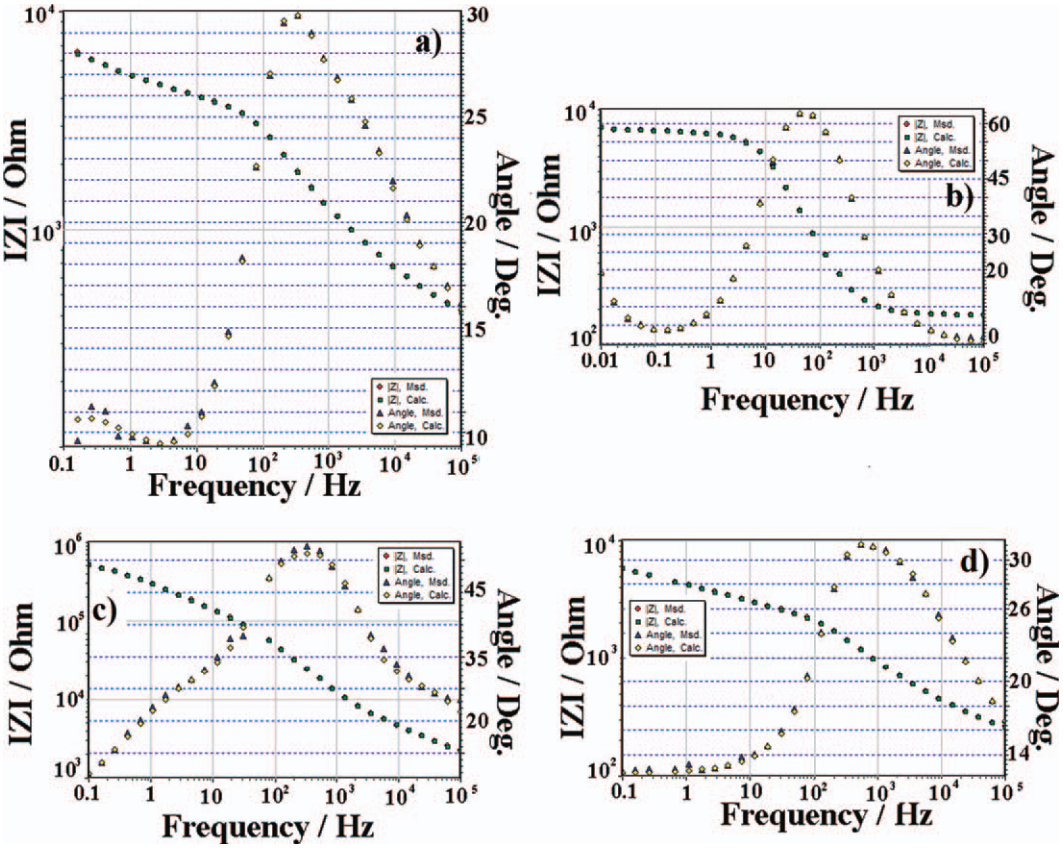

Figure 10 Bode-magnitude-phase plots of Poly(3MTh) on PET/ITO, (a) 0.1*M* $LiClO_4$/ACN and (b) 0.1*M* $NaClO_4$/ACN, (c) 0.1*M* $TBABF_4$/ACN, (d) $TEABF_4$/ACN, $[3MTh]_0$ = 10 m*M*. EIS measurements were conducted in monomer-free electrolyte solution with a perturbation amplitude 10 mV over a frequency range of 10 mHz to 100 kHz. [Color figure can be viewed in the online issue, which is available at wileyonlinelibrary.com.].

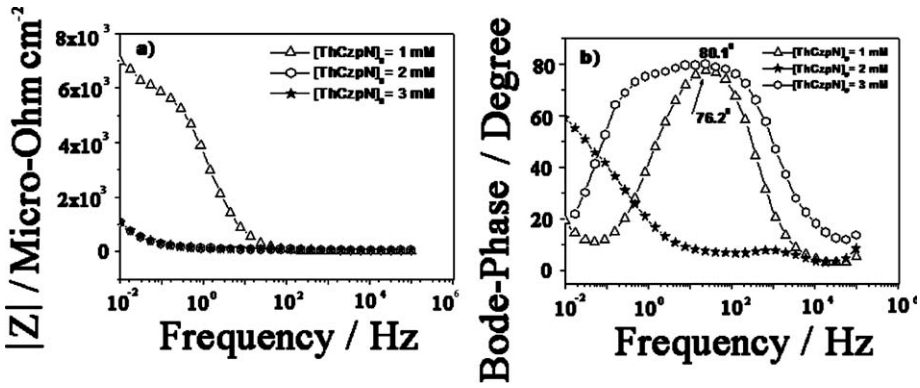

Figure 11 (a) Bode-magnitude and (b) Bode-phase plots for poly(ThCzpN) electrocoated on CFMEs. Plots were taken for $[ThCzpN]_0 = 1$, 2, and 3 m*M*.

0.75 value from $NaClO_4$ compared to $n = 0.37$ for $LiClO_4$, $n = 0.48$ for $TBABF_4$, and $n = 0.29$ for $TEABF_4$.

The copolymer film obtained from the electrolyte solution for $[ThCzpN]_0 = 1$ give the highest C_{dl} (0.334 mF cm^{-2}). However, the lowest double layer capacitances (C_{dl}) were obtained as 0.013 μF cm^{-2} for $[ThCzpN]_0 = 2$ and 3 m*M*, respectively [Fig. 11(a)]. The highest phase angles were obtained ~ 80.1° at the frequency of 23.89 Hz for $[ThCzpN]_0 = 3$ m*M* [Fig. 11(b)].

The highest conductive polymer of poly(3MTh) was obtained in 0.1*M* $NaClO_4$/ACN ($Y'' = 8.8$ mS cm^{-2}) [Fig. 12(b)]. The other conductivity results were obtained as 2.4 mS cm^{-2} for $LiClO_4$/ACN [Fig. 12(a)]; 0.8 mS cm^{-2} for $TBABF_4$/ACN [Fig. 12(c)]; 4 mS cm^{-2} for $TEABF_4$/ACN [Fig. 12(d)].

The conductivity values of poly(ThCzpN) were obtained from Admittance graph as ~ 90 mS cm^{-2} for $[ThCzpN]_0 = 1$ m*M*, ~ 10 mS cm^{-2} for $[ThCzpN]_0 = 3$ m*M*, ~ 5 mS cm^{-2} for $[ThCzpN]_0 = 2$ m*M* as shown in Figure 13.

EIS data were obtained for poly(3MTh) modified on PET/ITO at ac frequency varying between 0.01 Hz and 100 kHz with an applied potential in the region corresponding to the four different

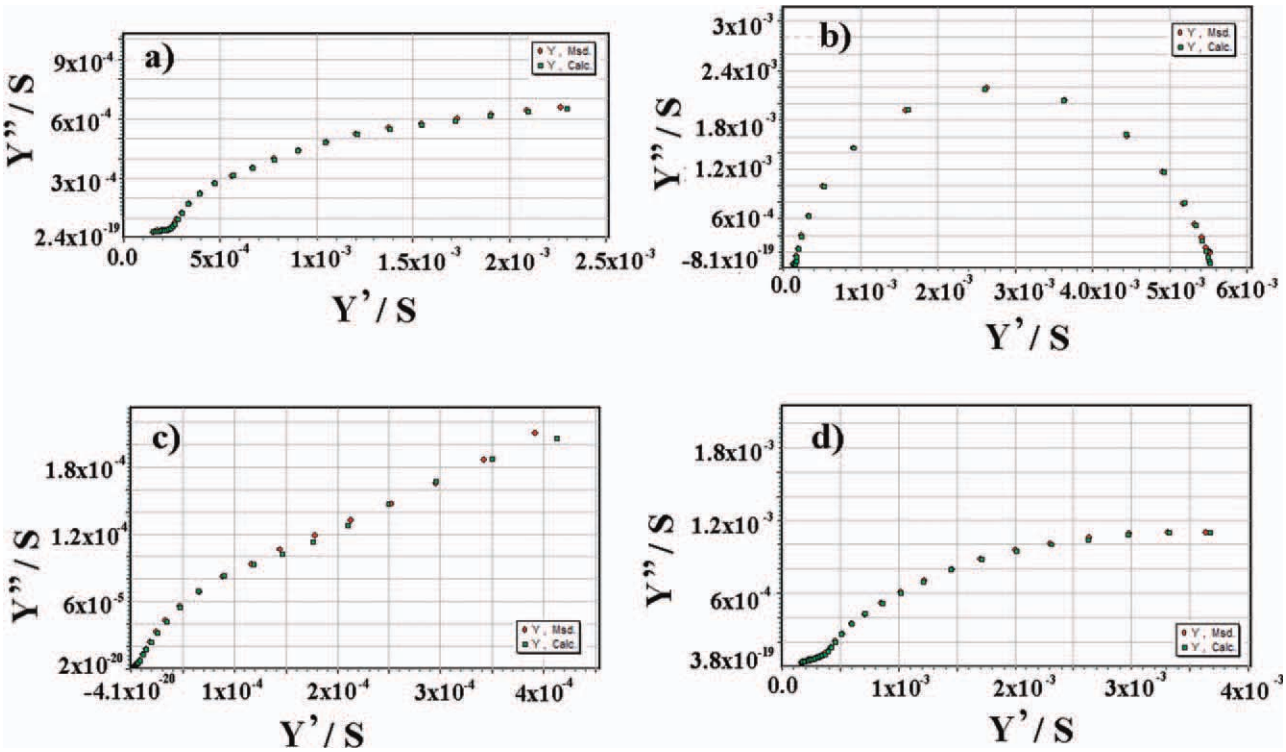

Figure 12 Admittance plots of Poly(3MTh) on PET/ITO, (a) 0.1*M* $LiClO_4$/ACN, (b) 0.1*M* $NaClO_4$/ACN, (c) 0.1*M* $TBABF_4$/ACN, and (d) $TEABF_4$/ACN, $[3MTh]_0 = 10$ m*M*. EIS measurements were conducted in monomer-free electrolyte solution with a perturbation amplitude 10 mV over a frequency range of 10 mHz to 100 kHz.

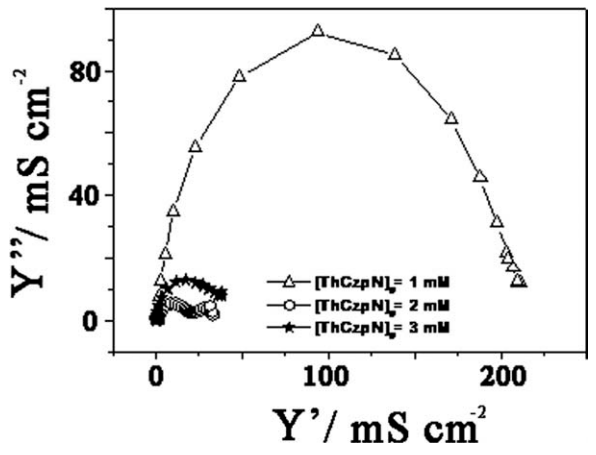

Figure 13 Admittance plot for poly(ThCzpN) electrocoated on CFMEs. Plots were taken for $[ThCzpN]_0 = 1$, 2, and 3 m*M*.

electrolytic solution. It was examined in equivalent circuit modeling of R(QR(CR)(RW))(CR) as shown in Figure 14.

The electrochemical parameters of the PET/ITO/poly(3MTh)/Electrolyte system were evaluated by given ZSimpWin program. In all cases the experimental data will be compared to an "equivalent circuit" that uses some of the conventional circuit elements, namely: resistances (R_s, R_1, R_2, R_3, and R_4), capacitances (C_1 and C_2), diffusion and induction elements. In this circuit, R_s is the solution resistance. Capacitors in EIS experiments often do not behave ideally; instead they act like a constant phase element (Q_1). C_1 and C_2 represent the capacitance of the double layer. Diffusion can create impedance known as the Warburg impedance, W.[43] R_s is almost within the limits of the experimental errors. In other words, the ionic/electronic charge transfer resistance, Q_1, shows gradual increase than decrease in value within the applied potential indicating that the migration of ionic species within the film pores is not the only mean of change-exchange at the polymer/electrolyte interface. This is also observed with the relative change in the value of the Warburg impedance, W. It changes accordingly with the charge transfer resistances. The circuit elements of poly(3MTh) can be compared as shown in Table I.

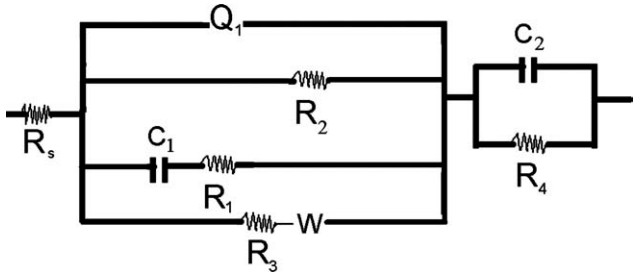

Figure 14 Circuit model of R(QR(CR)(RW))(CR).

TABLE I
Electrochemical Impedance Spectroscopic Results of Poly(3MTh) on PET/ITO Electrode by Means of Circuit Model, R(QR(CR)(RW))(CR)

Circuit component	$LiClO_4$	$NaClO_4$	$TBABF_4$	$TEABF_4$
χ^2	9.32×10^{-5}	1.21×10^{-4}	5.2×10^{-4}	5.29×10^{-5}
R_s/Ω	207.4	180.4	828.2	999
Q/F	2.8×10^{-5}	2.7×10^{-5}	9.9×10^{-7}	2×10^{-4}
n	0.37	0.75	0.48	0.29
R_1/Ω	8686	9476	6620	6381
C_1/F	5.4×10^{-9}	6.5×10^{-9}	3.7×10^{-9}	6.8×10^{-9}
R_2/Ω	4903	2728	1948	4963
R_3/Ω	5562	1.4×10^{4}	6.9×10^{5}	2763
$W/\Omega s^{-1/2}$	9.8×10^{-5}	3.9×10^{-5}	2.3×10^{-5}	5.7×10^{-6}
C_2/F	1.1×10^{-6}	4.4×10^{-6}	1.42×10^{-7}	1.23×10^{-6}
R_4/Ω	1329	3951	2500	665.7

CONCLUSION

Poly(3MTh) on PET/ITO was investigated by EIS technique in four different electrolytes such as $LiClO_4$, $NaClO_4$, $TBABF_4$, and $TEABF_4$ in ACN solvent. After electro-coating of monomer on PET/ITO, modified electrode was inserted in various monomer-free electrolyte solutions. Poly(3MTh) film has shown thin layer or diffusion controlled redox behavior. The EIS results were taken from 10 mHz to 100 kHz in these four different monomer-free solution. The EIS results are fitted to equivalent circuit model of R(QR(CR)(RW))(CR). C_{LF}, C_{dl}, phase angle, and conductivity values were calculated with the help of Nyquist, Bode-magnitude, Bode-phase and admittance graphs, respectively. The highest admittance ($Y' = 8.8$ mS cm^{-2}), maximum phase angle ($\sim 62.3^\circ$ at the frequency of 50 Hz), $C_{dl} = 17.6$ μF cm^{-2} and $C_{LF} = 59.1$ mF cm^{-2} values were obtained in $NaClO_4$/ACN medium for poly(3MTh) on PET/ITO. And also poly(ThCzpN)/CFME was studied in various initial monomer concentrations (1, 2 and 3 mM). The highest low-frequency capacitances (0.070 mF cm^{-2}) and phase angle (80.1°) for $[ThCzpN]_0 = 3$ mM. And the highest double layer capacitance and conductivity were obtained for $[ThCzpN]_0 = 1$ as 0.334 mF cm^{-2} and ~ 90 mS cm^2, respectively.

The authors wish to thank Prof. Dr. A. Sezai Sarac (Istanbul Technical University, Electropol. Laboratory, Istanbul, Turkey) for opportunity to use laboratory facilitates and Ozlem Oskan (Afyon Kocatepe University, Technology and Research Center (TUAM), Afyon, Turkey) for recording the SEM-EDX analysis.

References

1. Hong, S. Y.; Marnick, D. S. Macromolecules 1992, 25, 4652.
2. Guimard, N. K.; Gomez, N.; Schmidt, C. E. Prog Polym Sci 2007, 32, 876.

3. Tourillon, G.; Garnier, F. J Electrochem Soc 1983, 130, 2042.
4. Zotti, G. In Handbook of Electronic and Photonic Materials and Devices, Vol.8; Nalwa, H. S., Ed.; Academic: San Diego, 2000, p209.
5. Zen, A.; Saphiannikova, M.; Neher, D.; Asawapirom, U.; Scherf, U. Chem Mater 2005, 17, 781.
6. Elsenbaumer, R. L.; Jen, K. Y.; Oboodi, R. Synth Met 1986, 15, 169.
7. Jen, K. Y.; Miller, G. G.; Elsenbaumer, R. L. J Chem Soc Chem Commun, 1986, 17, 1346.
8. Ates, M. Int J Electrochem Sci 2009, 4, 980.
9. Bobacka, J.; Lewenstam, A.; Ivaska, A. Talanta, 1993, 40, 1437.
10. Mazur, M. Thin Solid Films 2005, 472, 1.
11. Skompska, M. Electrochim Acta 1998, 44, 357.
12. Hagen, G.; Thoresen, A. H.; Sunde, S.; Hesjevik, S. M.; Odegord, R. Mol Cryst Liq Cryst 1990, 189, 213.
13. Zhang, W.; Dong, S. J Electroanal Chem 1990, 284, 517.
14. Ates, M. Int J Electrochem Sci 2009, 4, 1004.
15. Eguílaz, M.; Agüí, L.; Yáñez-Sedeño, P.; Pingarrón, J. M. J Electroanal Chem 2010, 644, 30.
16. Chang, C.-C.; Her, L.-J.; Hong, J.-L.; Ho, W.-L.; Liu, S.-J. J New Mater Electrochem Syst 2008, 11, 49.
17. Taylor, D. M.; Gomes, H. L.; Underhill, A. E.; Edge, S.; Clemenson, P. I. J Phys D Appl Phys 1991, 24, 2032.
18. Mikayama, T.; Matsuoka, H.; Ara, M.; Uehara, K.; Sugimoto, A.; Mizuno, K. Sol Energy Mater Sol Cells 2001, 65, 133.
19. Marque, P.; Roncali, J.; Garnier, F. J Electrochem Soc 1987, 218, 107.
20. Refaey, S. A. M. Synth Met 2004, 140, 87.
21. Chen, Z. B.; Li, L. D.; Zhao, H. T.; Guo, L.; Mu, X. J. Talanta 2011, 83, 1501.
22. Mark, E. O.; Bernard, T. Electrochemical Impedance Spectroscopy; Wiley: Hoboken, NJ, 2008, p2.
23. Agrisuelas, J.; Garcia-Jareno, J. J.; Gimenez-Romero, D.; Vicente, F. Electrochim Acta 2010, 55, 6128.
24. Lin, Y.-S.; Chen, P.-W.; Lin, D.-J.; Chuang, P.-Y.; Tsai, T.-H.; Shiah, Y.-C.; Yu, Y.-C. Surf Coat Technol 2010, 205, S216.
25. Lin, Y.-S.; Chen, H.-T.; Lai, J.-Y. Thin Solid Films 2009, 518, 1377.
26. Lin, Y.-S.; Chen, P.-W.; Lin, D.-J. Thin Solid Films 2010, 518, 7416.
27. Lin, Y.-S.; Chiang, Y.-L.; Lai, J.-Y. Solid State Ionics 2009, 180, 99.
28. Li, S.-K.; Chou, J.-C.; Sun, T.-P.; Hsiung, S.-K. Biomed Eng Appl Basis Commun 2009, 21, 411.
29. Miettunen, K.; Halme, J.; Vahermaa, P.; Saukkonen, T.; Toivola, M.; Lund, P. J Electrochem Soc 2009, 156, B876.
30. Sarac, A. S.; Sezgin, S.; Ates, M.; Turhan, C. M. Surf Coat Technol 2008, 202, 3997.
31. Ates, M.; Yilmaz, K.; Shahryari, A.; Omanovic, S.; Sarac, A. S. IEEE Sens J 2008, 8, 1628.
32. Sarac, A. S.; Sezgin, S.; Ates, M.; Turhan, C. M. E. Adv Polym Technol 2009, 28, 120.
33. Ates, M.; Uludag, N.; Sarac, A. S. Fibers Polym 2011, 12, 8.
34. Ates, M.; Uludag, N. Fibers Polym 2010, 11, 331.
35. Tranvan, F.; Henri, T.; Chevrot, C. Electrochim Acta, 2002, 47, 2927.
36. Abdelrahman, H. A. Thin Solid Films 1997, 310, 208.
37. Robberg, K.; Paasch, G.; Dunsh, L.; Ludwigs, S. J Electroanal Chem 1998, 443, 49.
38. Sahok, E.; Vieil, E.; Inzelt, G. J Electroanal Chem 2000, 482, 168.
39. Rusling, J. F.; Suib, S. L. Adv Mater 1994, 6, 922.
40. Sarac, A. S.; Dogru, E.; Ates, M.; Parlak, E. A. Turk J Chem 2006, 30, 401.
41. Sarac, A. S.; Ates, M.; Parlak, E. A.; Turcu, E. F. J Electrochem Soc 2007, 154, D283.
42. Sarac, A. S.; Gilsing, H.-D.; Gencturk, A.; Schulz, B. Prog Org Coat 2007, 60, 281.
43. Atta, N. F.; El-Kady, M. F. Talanta 2009, 79, 639.